Computer Physics Communications

Application of Nuclear Reaction Analysis for aging investigations of detectors

G.Gavrilov, A.Krivchitch*, V.Lebedev

Petersburg Nuclear Physics Institute, Russian Academy of Science,

188300 Gatchina, St. Petersburg district, Russia.

Elsevier use only: Received date here; revised date here; accepted date here

Abstract

The article presents a thorough discussion of the applications of the Nuclear Reaction Analysis (NRA) method for investigating aging effects in gas-filled detectors. This technique is particularly efficient in a quantitative evaluation of the presence of light elements (oxygen, carbon, nitrogen, etc.) in the gold coating of the anode wire. The NRA method is also adequate for determining light element distribution with a depth measurement over a range of more than 1 μm. Such data are especially important in studies of gas-discharge avalanche plasmas because they are a starting point for most aging processes. The sensitivity of NRA to these elements is very high – about 5×10^{-2} %. Application of NRA in our aging investigations gave us a reliable confirmation of the key role of oxygen in the wire-swelling mechanism and demonstrated the kinetics of oxygen transport into the depth of the gold coating.

Keywords: aging; nuclear reaction analysis; quantitative evaluation.
*) Corresponding author: A.Krivchitch, E-mail address kriv@rec03.pnpi.spb.ru Fax (007)-812-71-37976; phone (007)-812-71-460-42.

1.Introduction

The study of physical and chemical phenomena taking place in thin films and near the surface of solids requires a quantitative determination and localization of trace elements within the depth of the material. Knowledge of the quantitative depth concentration provides information on diffusion phenomena, the radiation damage of an irradiated material, and the reemission of foreign atoms (carbon, nitrogen, oxygen, etc) from the environment [1, 2].

The nuclear physics methods using low-energy (1-3 MeV) proton and deuteron beams of electrostatic accelerators developed more than 30 years ago have been successfully applied for the purposes mentioned above [2, 3]. Nuclear Reaction Analysis (NRA) and Rutherford Backscattering Spectrometry (RBS) are used to investigate the element composition and the depth concentration profiles of atoms in thin films and the near-surface region of solids without their destruction. RBS is a good technique for obtaining quantitative elemental analysis in the near-surface region of materials [3]. However, analysis of low-Z elements (carbon, oxygen, etc), which are implanted into the matrix of medium and high-Z elements, is limited for this technique because the scattering cross-sections are proportional to Z^2. That is why oxygen may be detected only if that concentration is at least five times more than the concentration of gold [2, 3].

Therefore, the RBS technique can be used only for analysis of elements starting from calcium ($Z \geq 20$).

The NRA method proved to be more suitable for both detecting and quantitatively evaluating contents of oxygen and of other light-mass elements (lithium, boron, carbon, nitrogen, fluorine) as a function of depth in a heavy matrix, such as gold, tungsten, etc. [2, 3]. The principal advantage of NRA is that the detected reaction products usually have greater energy than particles elastically back-scattered from the heavy matrix. Thus the signal from the light element is detected in a range of the energy spectrum where the background is normally low.

We applied the NRA to investigate the depth concentration profiles of light elements (carbon, nitrogen, oxygen, fluorine, etc) in gold-plated tungsten wires with a diameter of 25 to 50 microns. These wires were used as anode wires in straw tubes that were subjected to aging tests. The total doses accumulated with the aged wires were up to 9 C/cm per wire. The drift tubes with these wires were operated with different gas mixtures, which contained gas components such as Xe, Ar, CO_2, and CF_4. The general principles of the NRA method are presented below.

2.Nuclear Reaction Analysis technique.

For detection and quantitative evaluation of carbon, nitrogen, and oxygen contents as a function of depth in the gold, the following nuclear reactions with deuterons were applied [2, 4-6]:

$$^{12}C + d \rightarrow {}^{13}C + p + Q_R \quad (1)$$

$$^{16}O + d \rightarrow {}^{17}O + p + Q_R \quad (2)$$

$$^{14}N + d \rightarrow {}^{15}N + p + Q_R \quad (3)$$

$$^{14}N + d \rightarrow {}^{12}C + \alpha + Q_R, \quad (4)$$

In these reactions, Q_R is the energy released in the reaction.

As one can see in Fig. 1a, these reactions do not have a resonance structure in the energy range of 0.7–1.1 MeV. To measure the fluorine concentration, we used a resonance nuclear reaction (Fig. 1b) with protons [2, 7]:

$$^{19}F + p \rightarrow {}^{16}O + \gamma + \alpha + Q_R. \quad (5)$$

The characteristics of the above-mentioned reactions at typical energy of deuterons and protons are presented in Table 1. These nuclear reactions demonstrate that the type and energy of emitted particles are characteristic of specific elements.

The reactions are exothermic, and thus the exiting protons and α-particles have higher energies than the incoming ions, which are impinging on the target. This allows us to absorb completely the beam ions with a few microns of aluminum foil placed in front of the semiconductor detector, which is used for detection of the final-state particles. Due to the Coulomb barrier, the energy of the bombarding ions is not sufficient for nuclear interaction with elements of higher atomic numbers (such as Al). Hence, the protons and α-particles produced in the interaction with light elements are detected practically without background. In the case of oxygen [4], a source of background could be competing nuclear reactions with other light nuclei, such as ^{11}B, ^{14}N, and Si. However, the correct choice of experimental conditions, such as beam energy and particle kinematics, allows easy rejection of the contribution of these reactions in the background.

2.1.Experimental set-up.

The NRA was carried out at the PNPI electrostatic accelerator with a maximum energy of 1.6 MeV [8]. The scheme of the experimental set-up is presented in Fig. 2. A frame holding the investigated wire was fastened to the target apparatus of a vacuum chamber. A deuteron beam of 0.9 MeV was used to analyze the oxygen distribution as a function of depth, while a 1.0 MeV beam was employed in the case of carbon and nitrogen, since the differential cross-sections of nuclear reactions have a plateau at these energies (Fig. 1a). The diameter of the beam spot on the wire was about 4 mm. The beam current through the wire was about 3-5 nA. The heat consumption of the irradiated wire was 0.01 - 0.02 W/cm. The number of deuterons that passed the wire was evaluated with the current integrator.

The nuclear reaction products (protons) were detected by a surface-barrier Si(Au) detector positioned at an angle of $\theta = 135^o$ to the beam axis. The acceptance area of the detector was 1.5 cm^2. The detector was located 6 cm from a sample. To suppress the background from the scattered deuterons, we shielded the detector with an aluminum foil with a thickness of 11 μm (3 mg/cm^2). The energy resolution of the spectrometer (Detector + Absorber) was $\Delta E = 50$ keV for $E_\alpha = 5.5$ MeV.

To measure the distribution of light elements along the wire, we scanned the target with the beam. The vacuum in the chamber was produced by a vacuum pump.

2.2. Technique of non-resonance nuclear reactions.

The method is based on the analysis of the energy spectra of emitted particles and makes it possible to determine a light-element concentration profile. Schematics and nomenclature for the (d,p) or (d,α) nuclear reaction processes in a sample target and the reconstruction of the resulting energy spectra are presented in Fig. 3. The energy spectra of the protons or α-particles produced by the (d,p)

or (d,α)-reactions at a constant energy of deuterons was measured using a semiconductor detector. No nuclear reaction occurs on the tungsten and gold nuclei themselves, due to the high value of atomic number Z.

The energy of a detected proton resulting from a reaction (d,p) at a depth t depends on the relationships between the beam particle energy and the path traveled by the emitted particles. A reaction that takes place near the surface of the specimen will yield protons with higher energy than a reaction that occurs at a greater depth.

The *energy-depth* relation may be deduced from the fact that the measured energy of a proton produced at depth t depends on the energy loss of deuterons reaching depth *t* and the energy loss of a proton in traversing the sample before it reaches the detector. To calculate this relation, a sample is sliced into thin layers with thicknesses Δt_i (Fig. 3). The energy of deuterons $E_d(t)$ with incident energy $E_d(0)$ at the depth t_1 is given by the following equation:

EQUATION MISSING HERE

Where $S_d(t)$ is the stopping power of a substance for deuterons and t_1 is the path length of deuterons in the target.

The energy $E_p(E_d)$ of protons resulting from a reaction (d,p) is given by the well-known kinematics expression [7]:

$$E_p(E_d(t)) = M_d \cdot M_p \cdot E_d \cdot \{2\cos^2\theta + B + 2\cos\theta \cdot [\cos^2\theta + B]^{1/2}\}/(M+M_p)^2 , \quad (7)$$

where $B = M \cdot (M+M_p) \cdot (Q_R/E_d - M_d/M + 1)/(M_d \cdot M_p)$, θ is the angle between the beam direction and the detector direction, and M_d, M_p, M are the masses of incident particle, outgoing particle, and final nucleus, respectively.

The energy of a proton in the detector $E_F(t)$ is given by presented below equation (8):

$$E_F(t) = E_p(E_d(t)) - \int_0^{t_2} \left| S_p(t) \right| dt - \int_0^{t_{Al}} \left| S_p(t_{Al}) \right| dt$$

where $S_p(t)$ is the stopping power of a substance for protons, $t_2 = t_1/\cos\theta$ is the path length of protons in the target, and t_{Al} the thickness of the aluminum foil-absorber.

Using tabulated stopping power data [9], the $E_F = E_F(t)$ dependence can be calculated from equations (6) – (8).

These calculations may be simplified because in our case the energy loss of particles is relatively small [9] compared with their initial energy (see Table 2).

This approximation appears to be quite reasonable if we take into account that the stopping powers have a linear dependence on the energy and vary less than 15 % over the relevant energy ranges: 0.7÷1.0 MeV for deuterons, 1.0÷1.6 MeV and 2.7÷3.1 MeV for protons.

In this case the energy scale can be converted into a linear depth scale. To a first order approximation, $E_p(t)$ can be expressed in the following way (9):

$$E_p(E(t)) = E_p(E_0) - (\partial E_p/\partial E_d) \times (E_0 - E_d(t)), \quad (9)$$

where E_0 is the deuteron energy in a beam.

$$E_F(t) = E_F(E_0) - G_{NR} \cdot t, \quad (10)$$

where $$G_{NR} = (\partial E_p/\partial E_d) \cdot S_d + S_p /\cos\theta. \quad (11)$$

Hence, according to equation (8) we have eq. (10), where G_{NR} is an effective energy loss related to a single length.

The derivative $(\partial E_p/\partial E_d)$ is calculated from eq. (7), and G_{NR} depends on energy losses of deuterons and protons, reaction kinematics, geometry of experiment, and elemental composition of investigated sample.

As shown in Fig. 3, we sliced the investigated sample into thin layers to provide the calculation. The thicknesses Δt_i are related to the energy intervals ΔE_i of the experimental spectrum via this equation:

$$\Delta t_i = \Delta E_i / G_{NR} \quad (12)$$

In order to demonstrate the good match between the exact calculation results and the linear approximation of the energy-depth relation, we have computed both approaches. The results obtained for a gold sample with 5% admixture of light nuclei (carbon; nitrogen and oxygen), produced in the reactions $^{12}C(d,p)^{13}C$, $^{14}N(d,p_5)^{15}N$, and $^{16}O(d,p_1)^{17}O$, are presented in Fig. 4. As indicated by the solid line, the linear approximation is practically valid for depths up to 2 mg/cm^2. For larger depths the approximation (10) is not correct (dashed line) due to an increase of the particle energy losses. In these cases the exact expression (6)-(8) must be used.

The ideal energy spectrum $Y(E_F)$ of the detected particles is given by the equation:

$$Y(E_F(t)) \cdot dE_F = C(t) \cdot I \cdot \sigma(E_d(t)) \cdot \Delta\Omega \cdot dt , \quad (13)$$

where C(t) is the concentration profile of the investigated element, i.e. the number of atoms of this element per cm^3 at the depth *t*; I is the number of incident particles; $\sigma(E_d(t))$ is the differential cross section for the angle θ; and $\Delta\Omega$ is the solid angle of a particle detection.

(6)

As one can see from (13), the number of proton counts $\Delta Y(\Delta E_F)$ in an energy interval ΔE_F of the experimental spectrum is proportional to the element concentration at depth *t* and to the reaction cross section for the energy of the deuteron at this depth $\sigma(E_d(t))$. The concentration profile can be computed if the excitation curve $\sigma(E_d)$ has already being measured, or by comparing with a sample containing a well-known element composition. Because of energy spread effects, the energy spectrum obtained experimentally is somewhat different from the one obtained from equation (13). The real spectrum can be computed from the convolution of the ideal spectrum $Y(E_F)$, the resolution function of the experimental system, and the straggling distribution [2].

To estimate the sensitivity of the NRA technique for the element concentration, we calculate the yield (Y) of particles emitted from an investigated sample with equation (13). These results are presented in Table 1. The required time T for a measurement is calculated as follows:

$$T = N_P / (Y \cdot I_B), \quad (14)$$

where N_P is the number of emitted particles reaching the detector. To obtain a precision of 3%, it is enough to collect just $N_P = 1000$ events;

Y [Counts/1μC] is the yield of emitted particles from a 1×10^{16} at/cm^3 surface layer of an element for a solid angle $\Delta\Omega = 0.1$ sr at $\theta = 135^0$; and

I_B [μA] is the beam current from the target (wire).

Taking into account that the beam current, collected from the thin anode wire, does not exceed $I_B = 0.01$ μA and Y = 28 Counts/ 1 μC, the time needed to collect the necessary statistics to measure the oxygen concentration at a level 1×10^{16} at/cm^3 in the gold matrix is quite reasonable at T = 60 min. It leads us to conclude that the sensitivity of the NRA technique for the element concentration measurements is about 1×10^{16} at/cm^2.

The accuracy of the element concentration measurements is determined by the following parameters:

- the accuracy of the beam intensity measurement, which is determined by the total charge measured with the current integrator, and does not exceed 3%;
- the accuracy of the known differential cross section for the considered nuclear reaction, which is estimated to be about 3% [4-6];
- inaccuracies in the geometry of the experiment ($\Delta\Omega$ and θ), which doesn't exceed 1%.

In total, the final accuracy of the element concentration measurements is better than 5%.

The thickness of the layer that can be investigated depends on the range of particles in the sample (for protons and deuterons) and in the absorber (for protons and α-particles). The thickness of the gold or tungsten that can be studied, as obtained from calculations, does not exceed 5-6 μm.

It is important to note that the effective energy loss in gold for protons and deuterons in the 0.5-3.0 MeV energy region are known with a precision up to 3 % [9].

The depth resolution δt of the method is determined by energy spread effects δE(t) related to the real experimental set-up and can be calculated from (12) as:

$$\delta t = \delta E(t) / G; \quad (15)$$

where

$$(\delta E(t))^2 = (\delta E_{spec})^2 + (\delta E_{beam})^2 + \\ +(\delta E_{geom})^2 + (\delta E(t)_{str})^2; \quad (16)$$

and δE_{spec} is the resolution function of the spectrometer; δE_{beam} is the energy resolution of the beam; δE_{geom} is the energy spread distribution due to the geometry of experimental set-up, and $\delta E_{str}(t)$ is the straggling distribution of particle energy in the sample.

The resolution function δE_{spec} of the spectrometer includes both the detector resolution, which is 25 keV for $E_\alpha = 5.5$ MeV, and the straggling distribution of energy δE_{str}(Al) in the aluminum absorber. The energy spread of the beam is very small and doesn't exceed $\delta E_{beam} = 0.1$ keV [8]. The spread δE_{geom} takes into account the dimensions of the detector, the distance between detector and sample (target), and the kinematics of the nuclear reaction. For our set-up we calculate $\delta E_{geom} = 16$ keV. For a near-surface region of a gold sample with thickness 2 mg/cm^2 (about 1 μm depth) the spread $\delta E_{str}(t)$ doesn't exceed 30 keV [2].

The contribution of δE_{str}(Al) was so strong that the final energy resolution of the spectrometer reached $\delta E_{spec} \cong 50$ keV for $E_\alpha = 5.5$ MeV.

Considering the *G* values that are presented in Table 1, it is clear that the NRA technique allows us to evaluate the light element content (oxygen) in the gold coating of the tungsten wire with a depth resolution better than 0.15 μm up to a depth of 1.0 - 1.2 μm. At depths of more than 2.5 mg/cm^2 the straggling contribution gets visible [2] and it needs to be taken into account in the analysis of the obtained data.

2.3.Technique of the resonance nuclear reactions.

As mentioned before, to investigate the fluorine content and depth profile in the sample, the resonance nuclear reaction $^{19}F(p,\alpha\gamma)^{16}O$ is used. This reaction has a very high resonant cross section at $E_{res} = 874$ keV and $E_{res} = 935$ keV with the widths $\delta E_{res} = 5.0$ keV and $\delta E_{res} = 8.6$ keV,

respectively (Fig. 1b) [7]. The energies of the emitted γ-rays are 6.13, 6.92 and 7.12 MeV.

The direct observation of the concentration profile can be obtained from nuclear reactions that exhibit a sharp resonance in the reaction cross section curve because the cross section σ(E) as a function of projectile energy E is negligible for off-resonance conditions with a narrow peak at a certain energy value $E_{res} \pm \delta E_{res}/2$. The experimental set-up for this nuclear reaction process in a sample is presented in Fig. 5.

The depth profiles are obtained by total yield measurements of γ-rays or α-particles step-by-step, with incident energies equal to and slightly higher than the resonance energy, i.e. by "shifting" the resonance through the sample. The energy resonance E_{res} and the proton beam energy E_b at depth t_{res} where this resonance occurs, are given by the equation:

$$E_{res} = E_b - \int_0^{t_{res}} \left(\frac{dE}{dt}\right)_p dt \qquad (17)$$

where $(dE/dt)_p$ is the energy losses of protons in the sample. The depth $t_{res,}$ where the resonance occurs, can be calculated from the following equation:

$$t_{res} = (E_b - E_{res})/(dE/dt)_p \qquad (18)$$

Since the energy dispersion of the beam particles in the electrostatic accelerator is much smaller than the resonance width (ΔE_{beam} = 100 eV at E_b = 1 MeV) [8], the depth resolution can be calculated as

$$\delta t = \Delta E_{res} / (dE/dt)_p \qquad (19)$$

The δt is equal to about 0.1 mg/cm^2 (Table 1). The intensity of the secondary particles (often γ photons) is proportional to the number of atoms of the element to be determined.

3. Electron technique for thin films investigation.

The analyses of anode surface after aging are usually performed using a scanning electron microscope with X-ray emission (0-10 keV) spectroscopy (SEM/XEM) [1, 10]. The SEM/XEM analysis yielded information on the morphology on the wire surface by imaging the scattered and secondary electrons, and on the atomic composition of a very thin surface layer by employing X-ray fluorescence spectroscopy. The SEM/XEM analysis has a good spatial resolution (less than 1 μm), but cannot provide the quantitative evaluation of the element content in the depth of the material. This is practically impossible because of the strong X-ray absorption by the wire material.

The attenuation of X-rays emitted by different elements in gold is presented in Table 3 [11]. It is seen that the attenuation power of X-rays of the light (carbon, nitrogen, oxygen and fluorine) and heavy (gold, tungsten) elements are quite different. The gold and the tungsten radiation can go out even from a depth of 1 μm of gold, while the light atom radiation could be detected only from very a thin upper layer (about 0.1 μm) of material. Moreover, identification of carbon is not a simple procedure, as it is likely that its signal (E_X = 0.28 keV) occurs in a region with high levels of background. The problem is that the secondary and scattered electrons, which are braking in the sample and the window of the detector, create a continuous background of bremsstrahlung. Its intensity, for instance, rises by more than ten times going in energy from 0.5 keV to 0.2 keV.

Due to the these reasons, one can conclude that XEM analysis cannot evaluate even the ratio between the light and heavy element contents.

4. Combination of different techniques for aging investigations.

A comparison of the SEM/XEM, Rutherford Backscattering Spectrometry (RBS) and Nuclear Reaction Analysis (NRA) methods is presented in Table 4. As one can see, the combination of these methods looks very promising to perform aging investigations of detector materials as these methods effectively complement each other. Parameters, which are of principal importance for each of the methods, are indicated by a gray background.

Experimental results, which clearly demonstrate the efficiency of the NRA method as applied in aging investigations, can be found in [12-15].

5. Conclusion.

1. The principle advantages of the Nuclear Reaction Analysis (NRA) are:

1.1. An opportunity to study, without etching, the depth profile of atomic composition for thin films and surface layers of solids. Thanks to ion braking the energy of the exiting particle gives the information about the depth where that reaction occurs. This method looks very promising and is unique due to its high sensitivity, the lack of etching, quantitative evaluation of the light element content, and the large depth reached.

1.2. This technique allows us to evaluate the light element content not only in the gold coating of a wire (~1 μm), but also in the tungsten.

1.3. The sensitivity of the proposed method for carbon, oxygen, and nitrogen is about $5 \cdot 10^{-2}$ %. The

precision of the quantitative evaluation of the element content depends on the accuracy of the known differential cross section for the considered nuclear reaction and is estimated to be about 5%.

2. Using the NRA method, in combination with SEM/XEM analysis, we can obtain much more precise and complete information about the aging processes in detectors.

3. From the NRA data in our aging investigations we inferred the following principle conclusions.

3.1. We demonstrated the key role of oxygen in the wire swelling mechanism and the kinetics of oxygen transport into the depth of the gold coating [12, 13].

3.2. The NRA method gave us an opportunity to detect unpredictable shape (or tail) distributions of the oxygen concentrations along the wire [14].

3.3. Measurement of the oxygen concentration in the gold coating can provide an excellent method to compare the aging resistance of different wires, which are intended to be used in gas-filled detectors under high accumulated dose.

Acknowledgements

We are very grateful to Prof. A. Vorobyov (PNPI) for his strong support of this work and the fruitful discussions of its results. We express thanks to V. Maleev (PNPI) and E. Ivanov (PNPI) for many fruitful discussions and help. We are very grateful to Jean-Michel Dalin (CERN) for his very friendly help in the SEM/XEM data analysis. We are very thankful to Yu. Lukjanov and V. Smolin for their kind help with the NRA of the obtained data.

References

[1] H.W.Werner, R.P.H.Garten, Rep. Prog. Phys. 47 (1984) 221.
[2] Ion beam handbook for material analysis, J.W.Mayer, E.Rimini,(eds.), Academic Press, New York, (1977).
[3] W.K.Chu, J.W.Mayer, M.A.Nicolet, Backscattering spectrometry, Academic Press, New York, (1978).
[4] G.Amsel, J.P.Nadai, E.D'Artemare, D.David, E.Girard, J.Moplin, Nucl. Instr. and Meth. 92 (1971) 481.
[5] M.Huez, L.Quaglia, G.Weber, Nucl. Instr. and Meth. 105 (1972) 197.
[6] J.A.Davies, T.E.Jackman, H.Platter, I.Bubb, Nucl. Instr. and Meth.218 (1983) 141.
[7] D.Dieumegard, B.Maurel, G.Amsel, Nucl. Instr. and Meth. 186 (1980) 93.
[8] V.M.Lebedev, Yu.G.Lukianov, V.A.Smolin, Proceedings of the "XIIIth International Conference on Electrostatic Accelerators", Obninsk, Russia, 25-28 May 1999 (2000) 60.
[9] J.F.Janni , Atomic Data and Nuclear Data Tables. 27(4/5) 348, 402 (1973).
[10] J.I. Goldstein, D.E. Newburg, P. Echlin "Scanning electron microscopy and X-ray microanalysis", Plenum Press, New York, (1981).
[11] W.M.J. Veigele, Atomic Data Tables, 5(1) (1973) 51.
[12] T.Ferguson, G.Gavrilov, A.Egorov, A.Krivchitch, E.Kuznetsova, V.Lebedev, L.Shipunov, Anode wire swelling - a possible phenomenon in anode wire aging under high-accumulated dose, accepted for publication in Nucl. Instr. and Meth. A, reference number 41300.
[13] T. Ferguson, G. Gavrilov, A. Krivchitch, E. Kuznetsova, V. Lebedev, L. Schipunov, The effect of oxygen on anode wire swelling under high-accumulated dose, Vienna Conference on Instrumentation 2001, Nucl. Instr. and Meth. A 478 (2002) 254.
[14] G. Gavrilov, A. Krivchitch, E. Kuznetsova, V. Lebedev, L. Schipunov, E. Lobachev, Aging investigation of the straw drift-tubes using Nuclear Reaction Analysis, Vienna Conference on Instrumentation 2001, Nucl. Instr. and Meth. A 478 (2002) 259.
[15] T. Ferguson, G. Gavrilov, V. Gratchev, A. Krivchitch, E. Kuznetsova, V. Lebedev, E. Lobachev, V. Polychronakos, L. Shipunov, and V. Tchrnjatin, Swelling phenomena in anode wires aging under a high accumulated dose, these proceedings.

Table 2. The stopping power of gold and aluminum for deuterons and protons.

Substance	E_d [MeV]	$\|S_d\|$ [keV/mg/cm^2]	E_p [MeV]	$\|S_p\|$ [keV/mg/cm^2]
Gold	0.9	95	1.6	51
Gold	1.0	90	3.0	38
Al (absorber)	-	-	1.6	130
Al (absorber)	-	-	3.0	80

Table 1. Nuclear reactions, which are used to measure carbon, nitrogen, oxygen, and fluorine content in the gold.

[a)] Yield/ 1μC from a $1\cdot10^{16}$ at/cm^2 surface layer of element for solid angle $\Delta\Omega = 0.1$ sr at $\theta=135^o$. Charge 1 μC corresponds to $6.25\cdot10^{12}$ particles for protons and deuterons.

Measured element	Types of nuclear reactions	Emitted Energy Q_R [MeV]	Beam Energy E_{beam} [MeV]	Thickness of the aluminum absorber in front of a detector t_{Al} [mg/cm^2]	Energy of emitted particles, $E_p(E_d(t=0))$ [MeV]	Effective energy loss, G_{NR}, [keV per mg/cm^2]	Depth resolution, δt [mg/cm^2]	Differential cross section, $d\sigma/d\Omega$ [mb/sr]	Yield [a)] Y [Counts per 1 μC]
C	$^{12}C(d,p)^{13}C$	2.72	1.0	3	3.0	114	0.44	30	180
N	$^{14}N(d,p_5)^{15}N$ $^{14}N(d,\alpha_0)^{12}C$ $^{14}N(d,\alpha_1)^{12}C$	1.30 13.6 8.14	1.0 1.0 1.0	3 3 3	1.8 10.0 6.8	170 270 360	0.31 0.19 0.14	6 0.07 1.1	35 0.4 5.9
O	$^{16}O(d,p_0)^{17}O$ $^{16}O(d,p_1)^{17}O$	1.92 1.05	0.9 0.9	3 3	2.4 1.6	165 180	0.3 0.28	0.74 4.5	5 28
F	$^{19}F(p,\alpha\gamma)^{16}O$	8.114	1.25	6	6.8 (α) and ~7 (γ)	$(dE/dt)_p$= =65keV/ mg/cm^2	0.1	0.5	3

Table 3. The attenuation of X-rays in gold.

Element	Energy of X-ray, E_x [keV]	Coefficient of attenuation, μ [μm^{-1}]	Attenuation $I(x) / I(0)=e^{-\mu \cdot x}$		
			x = 0.1 μm	x = 0.2 μm	x = 1 μm
Gold	2.2	2	0.82	0.67	0.091
Tungsten	1.8	3	0.74	0.55	0.050
Fluorine	0.68	17	0.18	0.033	$3.7 \cdot 10^{-8}$
Oxygen	0.52	23	0.10	0.01	$1.0 \cdot 10^{-10}$
Nitrogen	0.39	29.5	0.052	0.0027	$1.5 \cdot 10^{-13}$
Carbon	0.28	29	0.055	0.0030	$2.5 \cdot 10^{-13}$

Table 4. Comparison of the SEM/XEM, RBS and NRA methods for aging investigations of gold-coated tungsten wire.

Technical Characteristics		Different techniques for thin films investigation		
		Scanning Electron Microscopy with X-ray Emission Spectroscopy (SEM/XEM)	Rutherford Backscattering Spectrometry (RBS)	Nuclear Reaction Analysis (NRA)
Elements identified		C – U	Li – U	Li,Be,B,C,N,O,F
Morphology of surface		**Yes**	None	None
Lateral (space) resolution		**< 1 μm**	~3 mm	~3 mm
Sensitiviy	For the middle and heavy elements (Z> 20)	$=10^{15}$ at/cm^2 (in gold)	**$=1 \cdot 10^{12}$ at/cm^2 (in gold)**	The nuclear reactions for these nuclei are forbidden at this energy of ions
	For the light elements (Li, B, C, N, O, F) in the gold matrix	Only element Identification	$= 1 \cdot 10^{20}$ at/cm^2 (Oxygen in gold)	**$= 1 \cdot 10^{16}$ at/cm^2 (Oxygen in gold)**
Accuracy of the element concentration measurements		Only element identification	~ 5 %	**~ 5 %**
Thickness of investigated layers in the gold matrix		Not more than 0.1 μm(at the electron energy of 10 keV)	up to 6 μm	**up to 6 μm**
Depth resolution in the gold matrix		Equal to thickness of investigated layer	up to 0.1 μm	**up to 0.1 μm**
Depth analysis		Destructive	Non-destructive	**Non-destructive**

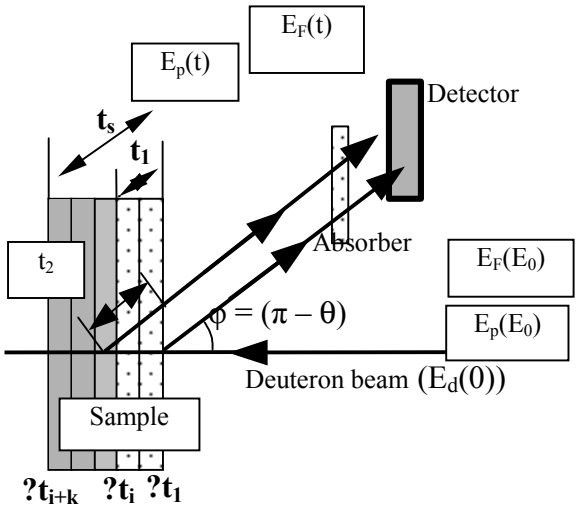

Fig.3. Schematics and nomenclature for the (d,p) nuclear reaction process in a sample.

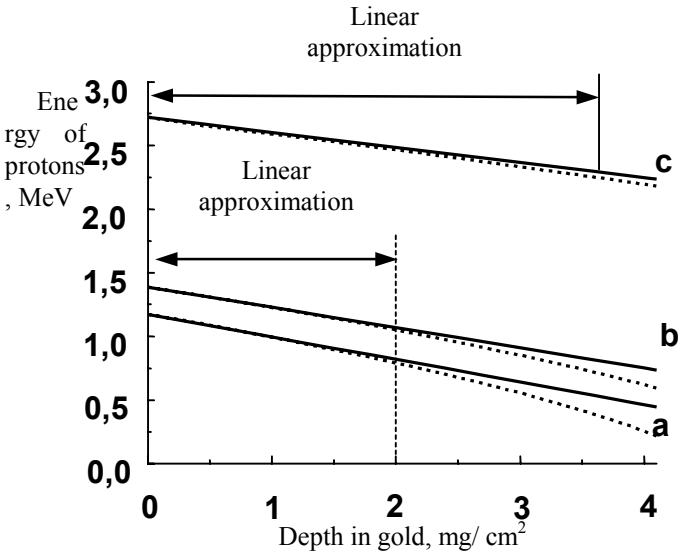

Fig. 4. Variation of the energy of the detected protons $\mathbf{E_F}$ with depth **t**, at which the $^{12}C(d,p)^{13}C$, $^{14}N(d,p_5)^{15}N$ and $^{16}O(d,p_1)^{17}O$ reactions take place (E_0=0.9 MeV, θ_{lab} = 135°), computed for the gold sample with 5% admixture of a light nucleus(**a** –oxygen, **b** – nitrogen, **c** –carbon). The calculation using G_{NR} is the continuous line. Exact calculations are dashed lines

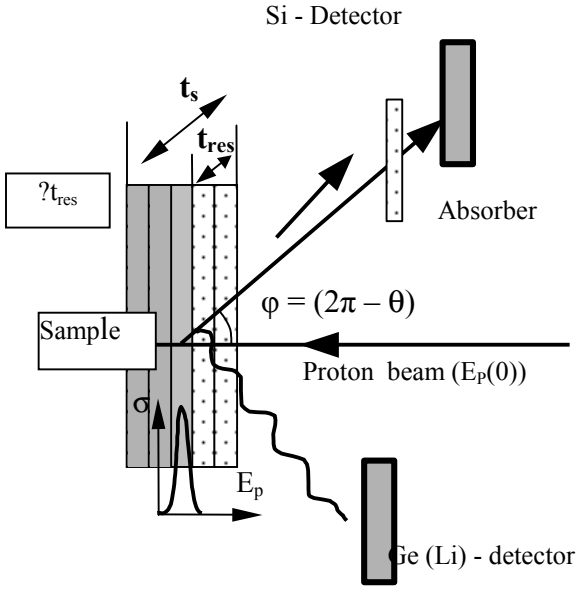

Fig.5. Schematics and nomenclature for resonance (p,αγ) nuclear reactions in a sample.

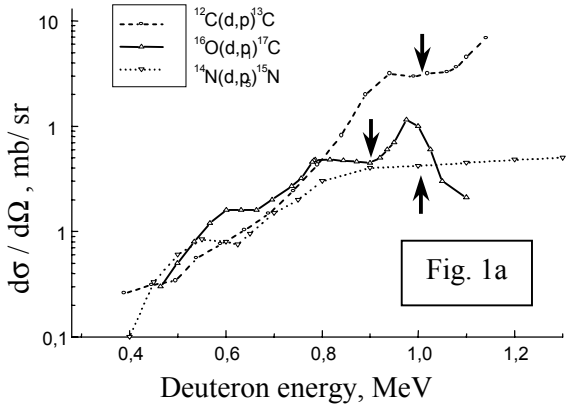

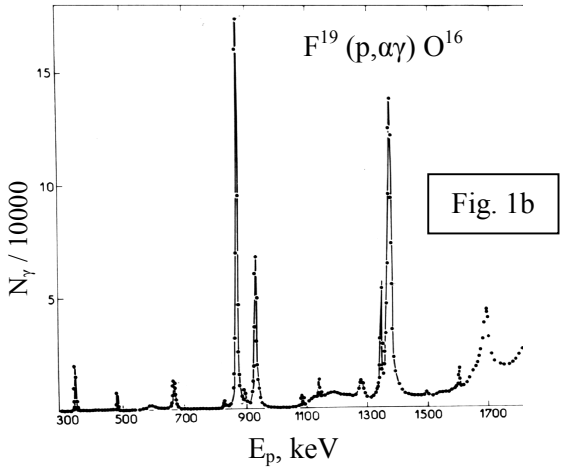

Fig. 1a. Cross section of the $^{12}C(d,p)^{13}C$ (dashed line), $^{14}N(d,p_5)^{15}N$ (dotted line) and $^{16}O(d,p_1)^{17}O$ (solid line) nuclear reactions at $\theta_{lab} = 135^o$ [4-6]. Arrows indicate the applied energies for carbon, nitrogen, and oxygen.

Fig. 1b. Overall view of the $^{19}F(p,\alpha\gamma)^{16}O$ excitation curve at $\theta_{lab} = 90^o$, normalized to a 3.8 μg/cm^2 fluorine target, 60 μC per point; 3" x 3" NaI(Tl) detector at 7 cm; detected $E_\gamma > 4.7$ MeV [7].

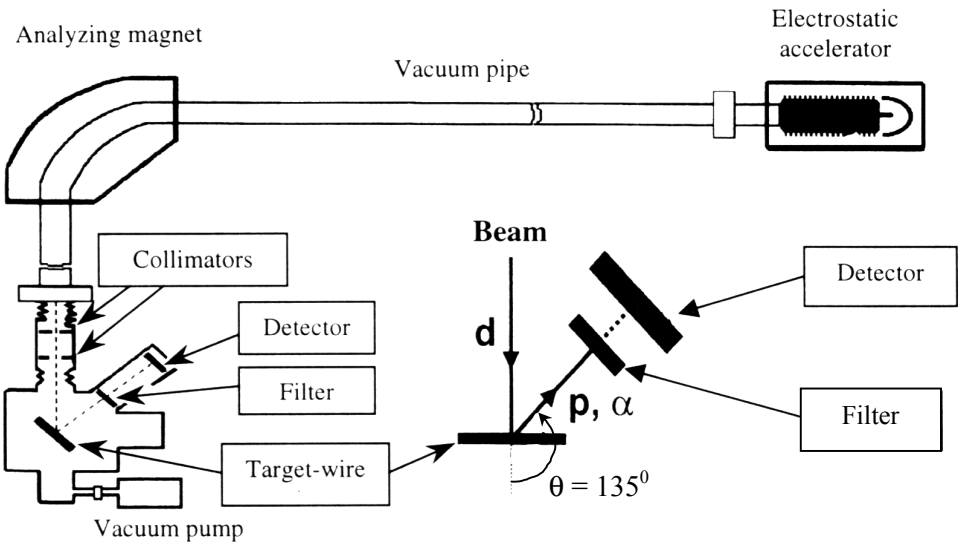

Fig.2. Schematic representation of the experimental set-up in the Nuclear Reaction Analysis.